Dispatch-Routing Optimization of Mobile Energy Storage for Spatiotemporal Arbitrage

Mukesh Gautam*, Li He*, Rakib Hossain*, Di Wu*, and Zhaoyu Wang†
*Pacific Northwest National Laboratory, Richland, WA, USA
†Electrical and Computer Engineering, Iowa State University, Ames, IA, USA

***Abstract*—Surging electricity demand, resource limitations, and transmission constraints are creating regional imbalances and congestion across power systems. Mobile energy storage (MES) offers a promising solution by enabling energy transfer among locations, improving resource adequacy and economic efficiency. This paper presents a mixed-integer linear programming framework for co-optimizing the dispatch and routing of MES to maximize spatiotemporal arbitrage revenue. The formulation incorporates a realistic transportation model that captures travel costs and time constraints, along with battery operational constraints and degradation considerations. The proposed method is illustrated and evaluated using 2020 locational marginal prices from NYISO and ISO-NE regions, combined with open-source routing data to represent realistic travel conditions across multiple spatial setups. Results show that mobility yields 7.9% to 9.6% higher revenues compared with stationary storage, with profitability shaped by the trade-off between regional price spreads and travel distances. A composite arbitrage potential score is also introduced to identify high-value locations, guiding MES deployment and investment decisions.**

***Index Terms*—Dispatch-routing optimization, economic assessment, mobile energy storage, spatiotemporal arbitrage, transportation modeling.**

I. Introduction

Surging electricity demand, limited transmission capacity, and resource constraints are creating regional imbalances and congestion across power systems. These challenges underscore the growing need for assets capable of addressing spatial and temporal supply-demand mismatches. While stationary energy storage systems have been widely adopted for grid support and market applications, their operation is confined to fixed locations, limiting their ability to address regional imbalances [1]. In contrast, mobile energy storage (MES) systems—typically composed of battery units mounted on transportable platforms—offer spacial flexibility by enabling movement among sites in response to regional congestion or spatial price variations [2]. Beyond traditional storage applications, MES systems can be strategically deployed for post-disaster grid restoration [3], temporary power supply to isolated areas, event-based or seasonal load support, and transmission congestion relief [4]. Their operational flexibility enables participation in multiple electricity markets, facilitating both grid support and economic optimization through location-based scheduling. Among these diverse applications, the potential for revenue maximization through spatiotemporal energy arbitrage—where storage assets are dynamically dispatched to exploit temporal and spatial price variations [5]—has emerged as a particularly promising area of research.

Existing studies on MES operation and scheduling have investigated a range of optimization strategies aimed at enhancing their technical and economic performance. A spatiotemporal decision model for utility-scale MES was developed and implemented in some regions in California [5]. Bi-level optimization frameworks have been developed to maximize MES revenue through joint capacity, routing, and dispatch optimization [6], while data-driven approaches using deep reinforcement learning have addressed MES arbitrage under uncertainty [7]. Additionally, particle swarm optimization approaches for MES energy management [8] and bi-level optimization models for MES operation within integrated transportation and power networks [9] have been proposed. While existing studies have established valuable foundations for MES scheduling, comprehensive evaluation of MES revenue potential driven by spatial and temporal price variations across multiple zones using real-world data remains relatively limited. Furthermore, the fundamental trade-offs between transportation costs and spatial price differentials that determine MES economic viability have not been systematically quantified in existing literature.

To bridge these gaps, this paper presents a mixed-integer linear programming (MILP) framework for MES revenue optimization through integrated spatiotemporal arbitrage. The model incorporates realistic operational and transportation constraints to identify optimal routing and dispatch across multiple market zones. In addition, a composite spatiotemporal arbitrage potential metric is developed to assist in selecting candidate locations with highest expected profitability, considering both temporal price volatility and inter-zonal price spreads. The effectiveness of the proposed framework is demonstrated through case studies using actual locational marginal prices (LMPs) from the New York Independent System Operator (NYISO) and ISO New England (ISO-NE) regions. By quantifying the fundamental trade-off between price spread magnitude and transportation distances, the framework provides key insights for optimal MES deployment strategies and establishes the foundation for strategic MES investments in competitive electricity markets.

The remainder of this paper is organized as follows: Section II presents the dispatch-routing optimization framework

This material is based upon work supported by the U.S. Department of Energy (DOE), Office of Electricity (OE), Energy Storage Division. Pacific Northwest National Laboratory is operated for DOE by Battelle Memorial Institute under Contract DE-AC05-76RL01830.

979-8-3315-8138-1

and mathematical formulation for revenue maximization. Section III details the case studies and comparative analyses using ISO-NE and NYISO data. Section IV provides concluding remarks and future work.

II. Modeling and Methodology

This section presents an MILP formulation that explores spatial arbitrage opportunities for revenue maximization, considering transportation and BESS operational constraints.

A. Problem Formulation

The proposed MES scheduling problem determines the optimal battery operation (charging/discharging) and movement across a predefined set of locations to maximize annual revenue. The optimization accounts for various factors and constraints, including spatial price differences, temporal price variations, transportation time and costs, BESS operational constraints and degradation.

1) Objective Function: The objective function maximizes net revenue as the difference between energy arbitrage revenue and transportation costs:

$$\begin{aligned} \max \quad & \Delta t \sum_{i\in\mathcal{L}} \sum_{t\in\mathcal{T}} \pi_{i,t}(P^{\mathrm{d}}_{i,t} - P^{\mathrm{c}}_{i,t}) \\ & - \sum_{i,j\in\mathcal{L}} \sum_{t\in\mathcal{T}} c_{\mathrm{trans}} d_{i,j} y_{i,j,t} \end{aligned} \tag{1}$$

where $\mathcal{L}$ is the set of locations, $\mathcal{T}$ is the set of time periods, Δt is the time step size, $\pi_{i,t}$ is the LMP, $P^{\mathrm{c}}_{i,t}$ and $P^{\mathrm{d}}_{i,t}$ are charging and discharging power, respectively, c_{trans} is the transportation cost per unit distance, $d_{i,j}$ is the distance between locations i and j, and $y_{i,j,t}$ is a binary transition variable (1 = in transit, not available for charging or discharging).

2) Constraints: The proposed MES optimization framework includes multiple physical and operational constraints to ensure feasible and realistic operation.

- *Energy State Dynamics:* The battery energy balance equations represent how the energy state E_t (energy stored at the end of time step t) changes over time due to charging and discharging operation:

$$E_t = E_{t-1} + \sum_{i\in\mathcal{L}} \left(\eta^{\mathrm{c}} P^{\mathrm{c}}_{i,t} - \frac{P^{\mathrm{d}}_{i,t}}{\eta^{\mathrm{d}}} \right) \Delta t, \quad \forall t \in \mathcal{T} \tag{2}$$

  where η^{c} and η^{d} are charging and discharging efficiencies, respectively. Note that in this paper, the energy represents the usable energy instead of total energy in a battery.
- *Energy Balance Constraint:* The initial energy E_0 and final energy E_T are set to be equal to maintain energy neutrality and avoid end-of-horizon bias.

$$E_T = E_0 \tag{3}$$

- *Energy Capacity Limits:* The stored energy is bounded by the usable battery capacity $\bar{E}$:

$$0 \le E_t \le \bar{E}, \quad \forall t \in \mathcal{T} \tag{4}$$

- *Cycle Limit:* To prevent excessive battery degradation, the total energy throughput is limited to C_{limit} cycles:

$$\frac{1}{2} \sum_{i\in\mathcal{L}} \sum_{t\in\mathcal{T}} \left(P^{\mathrm{c}}_{i,t} \eta^{\mathrm{c}} + \frac{P^{\mathrm{d}}_{i,t}}{\eta^{\mathrm{d}}} \right) \Delta t \le C_{\mathrm{limit}} \bar{E} \tag{5}$$

- *Power Limits:* Charging and discharging are only allowed when the MES is assigned to a site, enforced through binary variables $x_{i,t}$ indicating operation at location i during time t:

$$P^{\mathrm{c}}_{i,t} \le \bar{P}^{\mathrm{c}} x_{i,t}, \quad \forall i \in \mathcal{L}, t \in \mathcal{T} \tag{6a}$$
$$P^{\mathrm{d}}_{i,t} \le \bar{P}^{\mathrm{d}} x_{i,t}, \quad \forall i \in \mathcal{L}, t \in \mathcal{T} \tag{6b}$$

  where $\bar{P}^{\mathrm{c}}$ and $\bar{P}^{\mathrm{d}}$ are the maximum charging and discharging power limits.
- *Location Exclusivity Constraints:* The MES can operate at most one location or be in transit:

$$\sum_{i\in\mathcal{L}} x_{i,t} \le 1 - \sum_{i,j\in\mathcal{L}} y_{i,j,t}, \quad \forall t \in \mathcal{T} \tag{7}$$

- *Transition Logic:* Binary arrival and departure indicators $z^{\mathrm{arr}}_{i,t}$ and $z^{\mathrm{dep}}_{i,t}$ maintain location transition consistency:

$$z^{\mathrm{arr}}_{i,t} - z^{\mathrm{dep}}_{i,t} = x_{i,t} - x_{i,t-1}, \quad \forall i \in \mathcal{L}, t \in \mathcal{T} \tag{8a}$$
$$\sum_{i\in\mathcal{L}} (z^{\mathrm{dep}}_{i,t} + z^{\mathrm{arr}}_{i,t}) \le 1, \quad \forall t \in \mathcal{T} \tag{8b}$$

- *Auxiliary Transition Logic:* The auxiliary binary variables $z^{\mathrm{aux}}_{i,t}$ ensure temporal consistency during multi-period transitions:

$$z^{\mathrm{arr}}_{i,t} - z^{\mathrm{aux}}_{i,t} = \sum_{j\in\mathcal{L}} (y_{i,j,t-1} - y_{i,j,t}), \quad \forall i \in \mathcal{L}, t \in \{2, \dots, T\} \tag{9}$$

- *Auxiliary Exclusivity Constraint:* At most one arrival or auxiliary indicator can be active per time period:

$$\sum_{i\in\mathcal{L}} (z^{\mathrm{arr}}_{i,t} + z^{\mathrm{aux}}_{i,t}) \le 1, \quad \forall t \in \mathcal{T} \tag{10}$$

- *Transition Activation Constraints:* Departures must correspond to active transitions:

$$\sum_{i\in\mathcal{L}} y_{i,j,t} \ge z^{\mathrm{dep}}_{j,t}, \quad \forall j \in \mathcal{L}, t \in \mathcal{T} \tag{11}$$

- *Multi-Period Transit Constraints:* When a transition from location i to location j is initiated at time t, the MES remains in transit for the entire travel duration $\tau_{i,j}$. Two cases are considered depending on whether the transition completes within the planning horizon.
  1) Transition completes within the planning horizon: The transit indicator $y_{i,j,t}$ must remain active for each subsequent time step until arrival. This ensures continuity of the in-transit state:

$$\begin{aligned} & y_{i,j,t+k} \ge y_{i,j,t+k-1} - y_{i,j,t}, \\ & \qquad \forall i,j \in \mathcal{L}, \forall t \in \mathcal{T}, \forall k \in \{1, 2, \dots, \tau_{i,j}\} \end{aligned} \tag{12}$$

2) Transition extends beyond the planning horizon: The MES cannot participate in charging or discharging during from t to the end of the planning horizon.

$$P^{\mathrm{c}}_{j,t} = P^{\mathrm{d}}_{j,t} = 0, \quad \text{if } t + \tau_{i,j} > T \tag{13}$$

The proposed scheduling framework can be adapted to model stationary operation by introducing constraints that restrict the MES to a fixed location $\ell^* \in \mathcal{L}$:

$$x_{\ell^*,t} = 1, \quad \forall t \in \mathcal{T} \tag{14a}$$
$$x_{i,t} = 0, \quad \forall i \in \mathcal{L} \setminus \{\ell^*\}, t \in \mathcal{T} \tag{14b}$$
$$y_{i,j,t} = 0, \quad \forall i, j \in \mathcal{L}, t \in \mathcal{T} \tag{14c}$$

B. Annual Assessment

To evaluate long-term profitability and utilization patterns, annual assessment is required to capture seasonal variations in price spreads, congestion, and mobility opportunities. However, a single year-long optimization is both computationally intractable and unrealistic, as future market and transportation conditions are unknown. Therefore, this paper adopts an iterative simulation framework, in which the year is divided into realistic scheduling windows (e.g., 24 hours) that are solved sequentially across the annual horizon. This approach achieves computational efficiency and practical implementability. The sequential framework is summarized as follows, where W denotes the total number of windows, H denotes the length of the scheduling horizon, and Δ_w denotes the step size between consecutive windows:

1) Initialize annual revenue accumulator and initial conditions
2) For each optimization window $w = 1, 2, \ldots, W$:
   a) Extract LMP data for $[w \times \Delta_w, (w \times \Delta_w + H)]$
   b) Solve the optimization with current initial conditions
   c) Record optimal decisions and accumulate revenue
   d) Update initial conditions from solution for next window
3) Calculate total annual performance metrics

III. Case Study and Results

The proposed optimization and assessment framework is evaluated using 2020 LMP data from multiple zones across NYISO and ISO-NE markets. This section presents the case study setup, implementation details, and comparative assessment of mobile versus stationary energy storage operations.

A. Case Study Setup

The case studies are designed to capture both intra-ISO and inter-ISO price variations that influence the spatiotemporal arbitrage potential, involving five load zones as shown in Fig. 1. Two spatial setups are developed:

- In Setup 1, four load zones within the NYISO territory are selected: Long Island (LNIL, Zone K), New York City (NYC, Zone J), Dunwoodie (DNWD, Zone I), and Millwood (MLWD, Zone H). These zones are located within the downstate New York region, which experiences significant congestion and price differentials.
- In Setup 2, the MLWD is replaced by Connecticut (CNCT, Zone 4004) from the ISO-NE region. Including a zone from a neighboring ISO introduces greater price diversity and allows examination of potential cross-ISO revenue opportunities resulting from higher LMP spreads.

Fig. 1. Geographic locations of the load zones analyzed in the NYISO and ISO-NE regions.

TABLE I
MES System Parameters

Parameter	Value
Battery Energy Capacity	3.0 MWh
Maximum Charge Rate	0.75 MW
Maximum Discharge Rate	0.75 MW
Charging/Discharging Efficiency	95%
Daily Cycle Limit	1.0 cycles/day
Initial Battery SOC	50%
Transportation Cost	\$0.20/mile
Average Vehicle Speed	45 mph

For each setup, the optimization framework is executed under two operation modes: stationary (fixed at one location) and mobile (able to relocate among selected zones). Note that the MES may conclude operations at any location, avoiding unnecessary return transportation costs. Comparative analysis is conducted to quantify the revenue improvements and operational benefits achieved through mobility.

B. System Parameters and Assumptions

The MES system parameters are based on commercially available battery-truck configurations and realistic operational constraints, as summarized in Table I. Hourly LMP data for the year 2020 are obtained from the public datasets of NYISO and ISO-NE.

Representative geographical coordinates for each selected zone are assigned based on major cities located near the centroid of those zones. Specifically, Hartford represents CNCT, Yorktown Heights represents MLWD, Yonkers represents DNWD, Manhattan represents NYC, and Hicksville represents LNIL. Geographic distances between locations are calculated using the Open Source Routing Machine (OSRM) API [10], which provides road-network-based distances rather

TABLE II
ANNUAL PERFORMANCE COMPARISON: MOBILE VS. STATIONARY

Setup	Net Revenue		Revenue Increase
	Stationary	Mobile	
1	\$20,156	\$21,748	7.90%
2	\$19,748	\$21,653	9.65%

than Euclidean approximations. Travel times are computed based on the average vehicle speed and converted to integer hours using the ceiling function to maintain compatibility with the discrete-time optimization framework. The MILP is implemented in Julia using JuMP and solved with HiGHS.

C. Illustrative 3-Day Operation

Fig. 2 shows the optimal MES operation and routing under Setup 2 for a representative period (October 31–November 2), illustrating how the proposed framework jointly coordinates charging, discharging, and relocation decisions in response to spatiotemporal price variations. Note that for the selected three days, the LMPs at NYC and DNWD are nearly identical, which is why the two curves overlap. Key operational characteristics and insights are summarized below.

- Price-responsive operation: The MES system demonstrates clear correlation between price spreads and operational decisions, charging during low-price periods and discharging during high-price periods.
- Strategic movement: Location changes occur primarily during periods of significant spatial price differentials, validating the economic logic of mobility decisions.
- Operational continuity: The MES resumes charging or discharging promptly after each relocation, indicating efficient coordination between transport scheduling and power dispatch decisions.
- Cycle constraint enforcement: Over the three-day horizon, the MES completes three full cycles, demonstrating that the imposed cycle limits effectively regulate operation and prevent excessive degradation.

D. Annual Assessment

Annual assessments were conducted for both stationary and mobile BESS under the two spatial setups. The stationary BESS serves as the baseline for comparison to quantify the economic benefits of mobility. The annual optimization results are summarized in Table II.

For both mobile and stationary BESS, initial locations are optimally selected during the first 24-hour window. For mobile storage, subsequent windows maintain operational continuity by beginning at the final operating location of the previous window, while locations remain fixed for stationary storage. Comprehensive analyses reveal that maximum revenue is achieved when the initial location is LNIL. The analysis was conducted for all initial locations and setups, the maximum revenue case for each configuration is used to calculate mobility benefits.

The results demonstrate varying mobility benefits between the two setups:

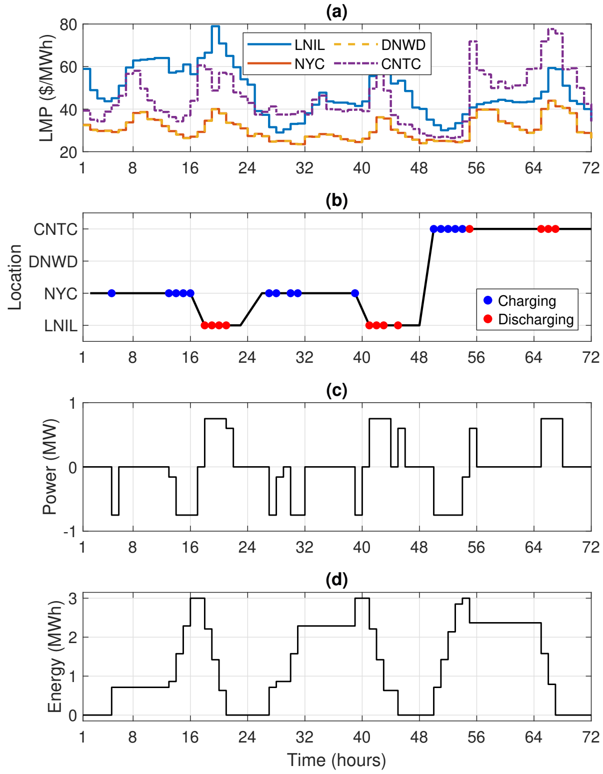

Fig. 2. MES operation over a representative 3-day period showing: (a) LMPs across all four locations, (b) operating location with charge/discharge status indicators, (c) net battery power with positive values indicating discharge and negative values indicating charge, and (d) battery energy evolution.

TABLE III
SPATIAL ARBITRAGE POTENTIAL ANALYSIS

Metric	Setup 1	Setup 2
Average Price Spread	\$7.43/MWh	\$8.62/MWh
Spread Volatility	\$8.46/MWh	\$8.56/MWh
High Spread Hours (>\$10/MWh)	1,978 (22.5%)	2,411 (27.4%)
Price Correlation Coefficient	0.933	0.899
Average Distance	33.4 miles	68.3 miles
Maximum Distance	56.8 miles	122.5 miles
Geographic Eff. (\$/MWh-mile)	0.223	0.126
Arbitrage Potential Score	0.876	0.913

- Setup 2 achieves a 9.65% revenue increase through mobility, while Setup 1 exhibits an increase of 7.90%.
- Setup 2 demonstrates superior mobility value despite slightly lower absolute mobile revenue.

E. Spatial Arbitrage Analysis

1) Arbitrage Potential Metrics: The spatial arbitrage potential of each setup is quantified through comprehensive analysis of price patterns and geographic efficiency, as shown in Table III. The metrics employed capture both temporal and spatial dimensions of arbitrage opportunities: average price spread ($\bar{\Delta\pi}$, mean hourly difference between maximum and minimum LMPs), spread volatility ($\sigma_{\Delta\pi}$, standard deviation of price spreads), high spread hours (H_{10}, frequency of periods exceeding \$10/MWh), price correlation coefficient (ρ, degree of price synchronization across locations), and geographic efficiency index (η_{geo}, ratio of average price spread to average distance). The arbitrage potential score (S_{arb}) is a composite metric combining all individual metrics into a single normalized indicator:

$$S_{\text{arb}} = 0.25\hat{\bar{\Delta\pi}} + 0.20\hat{\sigma}_{\Delta\pi} + 0.20\hat{H}_{10} + 0.15\hat{\rho}^{-1} + 0.20\hat{\eta}_{geo} \quad (15)$$

where normalized metrics are obtained by scaling each component to a 0-1 range relative to the maximum value across both setups, with the price independence term $\hat{\rho}^{-1}$ representing the normalized inverted correlation coefficient calculated as follows:

$$\hat{\rho}^{-1} = \frac{1-\rho}{\max(1-\rho)} \quad (16)$$

2) Key Findings: The arbitrage analysis reveals fundamental differences between the two setups:

- Setup 2 demonstrates higher average price spreads (\$8.62/MWh vs. \$7.43/MWh) and more frequent high-spread opportunities (27.4% vs. 22.5% of hours).
- Lower price correlation in Setup 2 (0.899 vs. 0.933) indicates greater spatial price independence and superior composite arbitrage potential score (0.913 vs. 0.876).
- Setup 1 achieves geographic efficiency advantages with compact footprint (33.4 miles vs. 68.3 miles average distance) and higher geographic efficiency index (0.223 vs. 0.126 \$/MWh-mile).
- Shorter inter-location distances under Setup 1 result in lower transportation costs despite more limited arbitrage opportunities.

F. Discussion

1) Arbitrage Potential vs. Geographic Efficiency Trade-off: The results reveal an interesting trade-off between overall arbitrage potential and geographic efficiency. Setup 2 achieves higher mobility benefits (9.65% vs. 7.90%) despite having a lower geographic efficiency index (0.126 vs. 0.223 \$/MWh-mile). This demonstrates that superior price spread characteristics and lower price correlation can compensate for increased transportation distances, as evidenced by higher arbitrage potential score (0.913) under Setup 2.

2) Distance-Price Spread Trade-off: The results demonstrate that revenue enhancement from mobility is governed by the complex interaction between price spread magnitude, price correlation, and transportation costs:

$$\text{Mobility Benefit} \propto \frac{\bar{\Delta\pi} \times (1-\rho)}{\bar{d}} \quad (17)$$

Setup 2 benefits from superior price spread characteristics ($\bar{\Delta\pi} = \$8.62$/MWh, $\rho = 0.899$) that outweigh the penalty of longer distances ($\bar{d} = 68.3$ miles), while Setup 1 achieves efficiency through geographic compactness ($\bar{d} = 33.4$ miles) but with more limited arbitrage opportunities ($\bar{\Delta\pi} = \$7.43$/MWh, $\rho = 0.933$).

3) Scalability and Economic Viability Considerations: While the observed 9.65% revenue enhancement represents a measurable improvement, the magnitude of spatiotemporal arbitrage benefits alone may not provide sufficient economic justification for widespread MES deployment. The relatively modest revenue increases highlight the need for value stacking that captures multiple value streams, such as resiliency and emergency response services, grid stabilization through ancillary service markets, transmission infrastructure deferral, and distribution-level capacity cost avoidance.

IV. Conclusion and Future Work

This paper presented a dispatch-routing optimization method for MES and evaluated its potential for spatiotemporal arbitrage using 2020 LMP from NYISO and ISO-NE regions. The proposed framework incorporates a realistic transportation model that captures travel costs and time constraints, along with battery operational constraints and degradation considerations. The case study results show that revenue enhancement from mobility is governed by the complex interaction between price spread characteristics, price independence, and transportation distances, with the introduced composite arbitrage potential score serving as effective predictors of mobility benefits. Across the evaluated setups, mobility increased annual revenues by 7.9–9.6%, representing a significant improvement over stationary operation and demonstrating that favorable price dynamics can offset longer travel distances when selecting optimal location sets. While these findings highlight the economic promise of mobility, spatiotemporal arbitrage alone may not be sufficient to justify large-scale MES deployment, highlighting the need for strategic siting to maximize arbitrage potential and value stacking from other value streams to ensure economic viability.

References

[1] Z. Yan, Y. Zhang, and J. Yu, "An allocative method of stationary and vehicle-mounted mobile energy storage for emergency power supply in urban areas," *Energy Storage*, vol. 6, no. 5, p. e681, 2024.

[2] Y. Yang, J. Qiu, and C. Zhang, "Distribution network planning towards a low-carbon transition: a spatial-temporal carbon response method," *IEEE Trans. Sustain. Energy*, vol. 15, no. 1, pp. 429–442, 2023.

[3] M. Gautam, N. Bhusal, and M. Ben-Idris, "Postdisaster routing of movable energy resources for enhanced distribution system resilience: a deep reinforcement learning-based approach," *IEEE Industry Applications Magazine*, vol. 30, no. 2, pp. 63–76, 2023.

[4] H. Abdeltawab and Y. A.-R. I. Mohamed, "Mobile energy storage sizing and allocation for multi-services in power distribution systems," *IEEE Access*, vol. 7, pp. 176 613–176 623, 2019.

[5] G. He, J. Michalek, S. Kar, Q. Chen, D. Zhang, and J. F. Whitacre, "Utility-scale portable energy storage systems," *Joule*, vol. 5, no. 2, pp. 379–392, 2021.

[6] K. Tian, Y. Zang, J. Wang, and X. Zhang, "Electricity arbitrage for mobile energy storage in marginal pricing mechanism via bi-level programming," *Int. J. Electr. Power Energy Syst.*, vol. 162, p. 110330, 2024.

[7] T. Chen, X. Xu, H. Wang, and Z. Yan, "Routing and scheduling of mobile energy storage system for electricity arbitrage based on two-layer deep reinforcement learning," *IEEE Trans. Transport. Electrific.*, vol. 9, no. 1, pp. 1087–1102, 2022.

[8] H. H. Abdeltawab and Y. A.-R. I. Mohamed, "Mobile energy storage scheduling and operation in active distribution systems," *IEEE Trans. Ind. Electron.*, vol. 64, no. 9, pp. 6828–6840, 2017.

[9] W. Sun, W. Liu, J. Zhang, and K. Tian, "Bi-level optimal operation model of mobile energy storage system in coupled transportation-power networks," *J. Modern Power Sys. Clean Energy*, vol. 10, no. 6, pp. 1725–1737, 2022.

[10] OSRM Project Team, "Open Source Routing Machine API Documentation," 2025. [Online]. Available: http://project-osrm.org/docs/v5.24.0/api/

979-8-3315-8138-1